BONE REMODELLING OF THE HUMERUS AFTER A SHOULDER ARTHROPLASTY

Carlos Quental
Nº 54212
e-mail: miguel@kental.net

Keywords: Biomechanics, glenohumeral joint, humerus, shoulder arthroplasty, bone remodelling, finite element method.

ABSTRACT

In this work computational models are developed to analyze bone remodeling of the humerus after a shoulder arthroplasty using either a cemented or press-fit stem. Bone is modelled as a porous material, characterized by its local density. The bone remodelling model is based on a global optimization criterion by the minimization of a function which takes into account both structural stiffness and the metabolic cost related with bone maintenance, by the use of a biomechanical parameter k that varies with different biological factors. The most suitable value for the biomechanical parameter k is chosen based on the analysis of three-dimensional models of the humerus without the implant, in order to achieve the one which best reproduces its real morphology. This way, not only the most appropriate value for k is defined but also the model is validated, showing its ability to reproduce with high similarity the real morphology of bone. After the determination of the biomechanical parameter k, the bone remodelling model was applied to the three-dimensional models of the implanted humerus, starting with the same density distribution as the obtained previously with the model of the humerus without the implant, being thus closer to reality. The results obtained, in general, do not show significant changes of the bone mass which leads to the conclusion that stress shielding and the resulting bone remodelling do not play a major role in the failure of the shoulder prosthesis.

1. INTRODUCTION

The glenohumeral joint (GHJ), often referred as the shoulder joint, presents the greatest mobility of any joint of the body. The GHJ is a synovial ball and socket joint, involving the articulation between the glenoid fossa of the scapula and the head of the humerus (Souza 2001) (Palastanga, Field e Soames 2000). However, in this particular joint, the humerus head does not fit perfectly within the glenoid because of its larger surface area resulting in an inherent instability. The lack of stability is compensated mostly by the rotator cuff, four muscles surrounding the joint, which provide the necessary stability by pressing the humerus against the glenoid.

The shoulder is the third most frequently replaced joint after the hip and knee (Norris e Iannotti 2002). The lack of range of motion and pain are the main reasons patients consider this operative treatment, whether resulting from osteoarthritis, the most common pathologic condition, rheumatoid arthritis, rotator cuff tear, avascular necrosis or fracture (Bigliani e Flatow 2005).

As in other joint replacements, several complications resulting from shoulder arthroplasty have been reported (Boshali, Wirth e Rockwood 2006) (Hasan, et al. 2002). Nevertheless, most reports only focus on the glenoid component so there is little material in literature about the humeral component, in particular about remodelling of the humerus

after the implantation of a humeral prosthesis. As, for example, in the hip joint, the insertion of a stem in the medulla of a long bone may change the distribution of load which consequently can cause the resorption of bone as a result of stress shielding (Nagels, Stokdijk e Rozing 2003). This way, stress shielding conditions the bone adaptation to the changed stress distribution following Wolff's law, resulting in a weaker bone which may lead to a higher risk of failure of the prosthesis.

The reported complications resulting from the humeral component are humeral loosening and perisprosthetic fracture. Amy K. Franta et. al. in a study of 282 unsatisfactory shoulder arthroplasties reported 31 cases, about 11%, of humeral loosening complications and 6 cases (2%) of periprosthetic fracture (Franta, et al. 2007). Kamal I. Boshali et. al. in a similar study found 27 cases of humeral loosening and 46 of periprosthetic fracture in 414 verified complications (Boshali, Wirth e Rockwood 2006). Samer S. Hasan et al. reported 17 cases (12%) of humeral loosening and 5 cases (4%) of periprosthetic fracture in 141 studied cases (Hasan, et al. 2002).

The purpose of the current work is to simulate and analyze bone remodelling of the humerus after implantation of a humeral prosthesis, using a finite element method, in order to identify possible causes for the failure of humeral components of shoulder arthroplasties.

2. METHODS

This section provides a simple description of the bone remodelling model used in the current work and a detailed explanation of the methodology taken.

2.1. Computational bone remodelling model

The bone remodelling model used in the present work is based on global optimization criteria. Considering bone to be an optimal structure, able to adapt itself in order to have the stiffest structure given the applied loads, this model combines a stiffness criterion with a biological cost parameter k that controls total bone mass (Fernandes, Rodrigues e Jacobs 1999).

Trabecular bone microstructure is obtained by the periodic repetition of a micro cubic cell with prismatic holes, with dimension a_1, a_2 and a_3 (Figure 1).

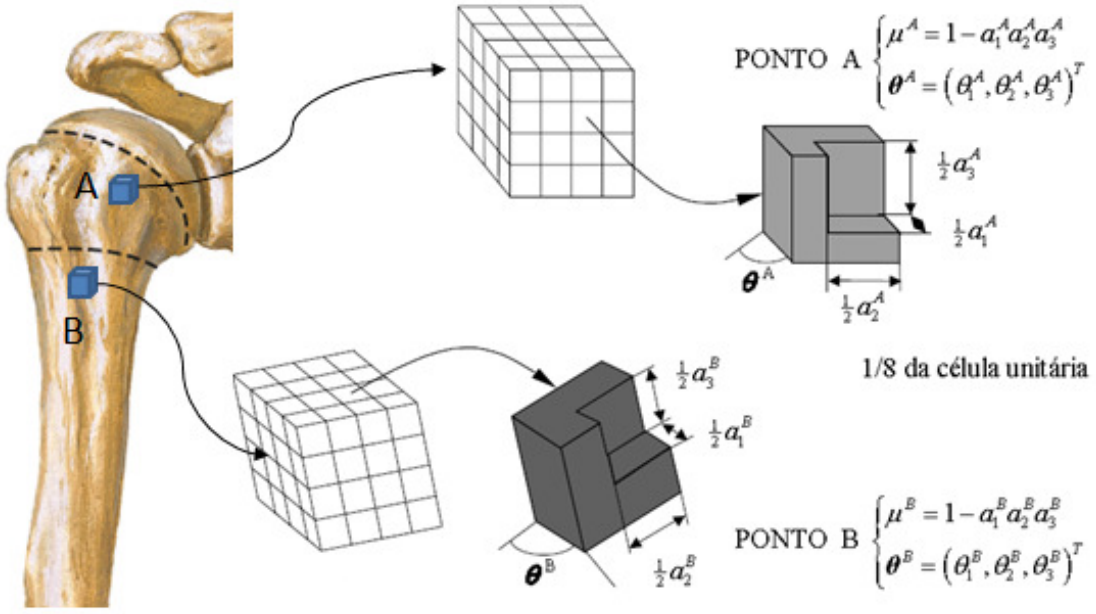

Figure 1 – Material model for trabecular bone

The relative density μ, the design variable, depends on the local hole dimensions, given by $\mu = 1 - a_1 a_2 a_3$.

The bone remodelling law may be stated by equation 1:

$$\sum_{P=1}^{NC}\left[\int_{\Omega_b} \alpha^P \frac{\partial E^H_{ijkl}}{\partial a} e_{kl}(u^P) e_{ij}(v^P)\delta a d\Omega\right] + \int_{\Omega_b} (\lambda_1 - \lambda_2)\delta a d\Omega + k\int_{\Omega_b} \frac{\partial \mu}{\partial a}\delta a d\Omega = 0, \forall a \quad (1)$$

where NC is the total number of load cases, each with weight factor α^P satisfying $\sum_{P=1}^{NC} \alpha^P = 1$, E_{ijkl} the material properties tensor and e_{ij} the strain field.

The material properties are obtained by the homogenization method. For a detailed description of the homogenization method see Guedes and Kikuchi's work (Guedes e Kikuchi 1990).

2.2. Computational models

The model described above was applied to three-dimensional models constructed using Solidworks. The humerus geometry was acquired at the Vakhum project database and, firstly, only the bone, with and without medullar cavity, was considered in order to infer the value for parameter k and also validate the bone remodelling model. Later on, two different prostheses, based on Zimmer implants, were modelled and the respective model assembled given rise to cement model and cementless model or press-fit model.

The finite element meshes were generated with Abaqus (Figure 3) and six load cases were applied (Favre, et al. 2005) with weight factors of (1/6). The muscular forces were applied as concentrated forces by the division of the resultant force and the number of nodes of each muscle, according to its anatomical attachment. The glenohumeral reaction forces were applied as pressures.

2.2.1. Parameter k determination

Using the model of the bone without implant, the most appropriate value for parameter k should present a bone structure with high similarity with the real humerus morphology. So, starting with a uniform density distribution of 0.3, different values for k were tested: $0.1 \times 10^{-3}, 0.2 \times 10^{-3}$ and 0.3×10^{-3} (Figure 2). The most adequate value seemed to be 0.2×10^{-3} since it was the most similar to the humerus morphology.

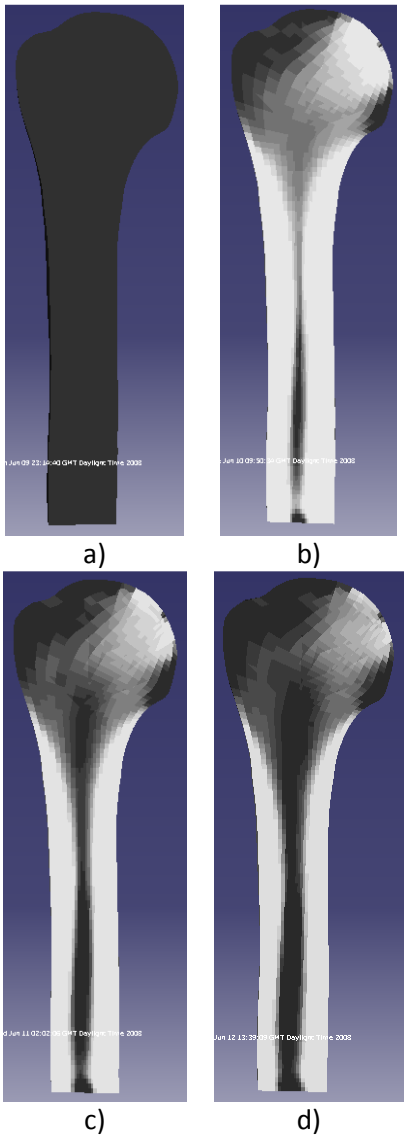

Figure 2 – Longitudinal section of the three-dimensional model of the intact humerus without medullary cavity. Densities presented in a gray scale, where gray is trabecular bone and white cortical bone. a) Initial distribution b) Final distribution for k 0.1×10^{-3} c) Final distribution for k 0.2×10^{-3} d) Final distribution for k 0.3×10^{-3}.

2.2.2. Implanted humeral models

Considering that the model of the bone without implant was able to reproduce the humerus morphology, the initial density distribution of the implanted models was considered to be the final density distribution of the intact bone model with medullary cavity, starting this way with a more realistic approach.

In the cemented model, the prosthesis is of Co-Cr alloy, with elastic modulus of 230 GPa and Poisson's ratio of 0.3 (Folgado 2004). The bone cement, the polimethyl methacrylate, was considered to have 2.1 GPa of elastic modulus and 0.4 of Poisson's ratio (Andreykiv, et al. 2005). For the contact problem, the cement was considered completely tied to the bone and the prosthesis–cement interface was split into three different cases: one where they are bonded (Jeffers, et al. 2007), other with frictionless contact and another with friction contact with friction coefficient of 0.3 (Mann, Ayers e Damron 1997).

In the press-fit model the prosthesis is made of two different materials. The stem is made of titanium while the head is made of Co-Cr alloy. The elastic modulus was considered to be 230 GPa for Co-Cr alloy and 115 GPa for titanium and the Poisson's ratio of 0.3 for both (Fernandes, et al. 2002). The bone–stem interface was modelled considering two different cases: one with frictionless contact and other where the stem is bonded to the bone, simulating a full osseointegration stem. To finish, a case with frictionless contact where the muscle action is omitted, was modeled. In fact, patients often present some level of muscle dysfunction, though this model reproduces an extreme situation. On the other hand, this model resembles finite element models of the hip, where the joint reaction is the main load (Huiskes, Weinans e Dalstra 1989).

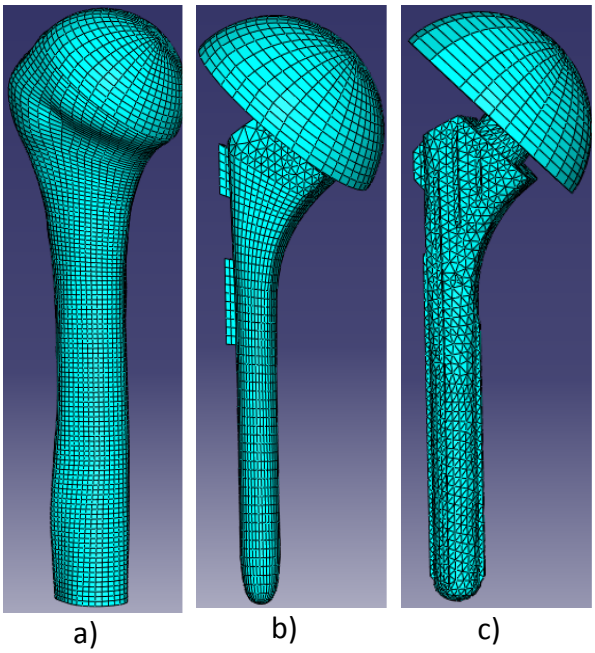

Figure 3 – Finite element meshes of the three-dimensional models. a) Implanted model b) Cemented stem c) Press-fit stem

2.2.3. Results Analysis

Since the bone remodelling process can be a difficult task to analyze by the comparison of two different images (initial and final density distribution), two other analysis methods have been followed. To begin with, a global analysis of the total bone mass was evaluated according to the total number of iterations. As the overall behaviour may not mean a good local description, the bone was also divided in 8 different zones (Figure 4) (Verborgt, El-Abiad e Gazielly 2007) (Sanchez-Sotelo, et al. 2001), where the relative evolution of the total density of the region is computed (equation 2) whether considering or not the interface elements.

$$Var(\%) = \frac{\left(\sum_{i=1}^{n} \rho_i^{final} \times V_i^{el} - \sum_{i=1}^{n} \rho_i^{initial} \times V_i^{el}\right)}{\sum_{i=1}^{n} \rho_i^{initial} \times V_i^{el}} \times 100 \quad (2)$$

where ρ is the relative density, V_i^{el} the volume of element i and n the total number of elements of a region.

This way one can have a better understanding of the bone remodelling process not only for the global structure of the bone but also for the different regions in contact with the stem.

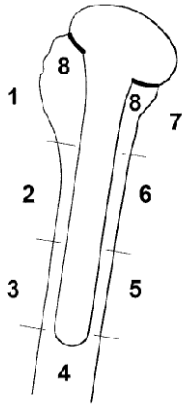

Figure 4 – The humerus was divided into 8 different zones

3. RESULTS

In this section, the bone remodelling results for the cemented and press-fit models are presented.

3.1. Cemented model

To begin with, Figure 5 presents the total bone mass evolution of the three cemented models. As it can be seen, only the bonded model presents global bone loss. It should be noted that despite the number of iterations, the bonded model did not stabilized as desired. However it is evident the model evolution, so more iterations would just emphasize the registered results.

The bone remodelling results are presented in Figure 7.

For a better understanding, Table 1 presents a discriminatory evolution of the different regions of the bone.

3.2. Press-fit model

As it was done in the cemented models the same analysis was also done for the press-fit models, beginning once more with the total bone mass evolution (the bonded model and the model without muscle action did not stabilized as desired) (Figure 6), then with the bone remodelling results (Figure 8) and finally the relative density evolution of the different regions of the humerus (Table 2).

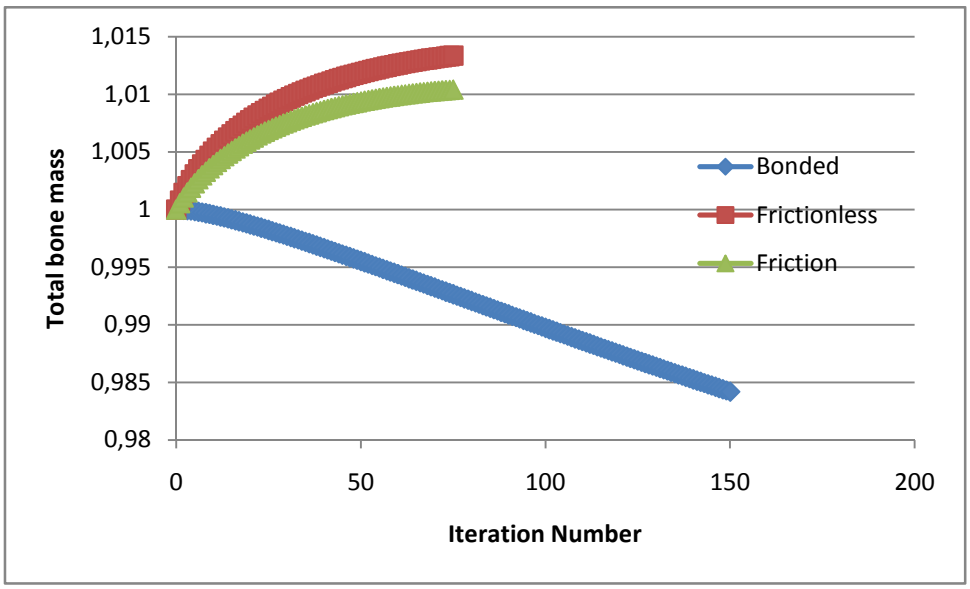

Figure 5 – Evolution of bone mass during the bone adaptation process for the cemented models

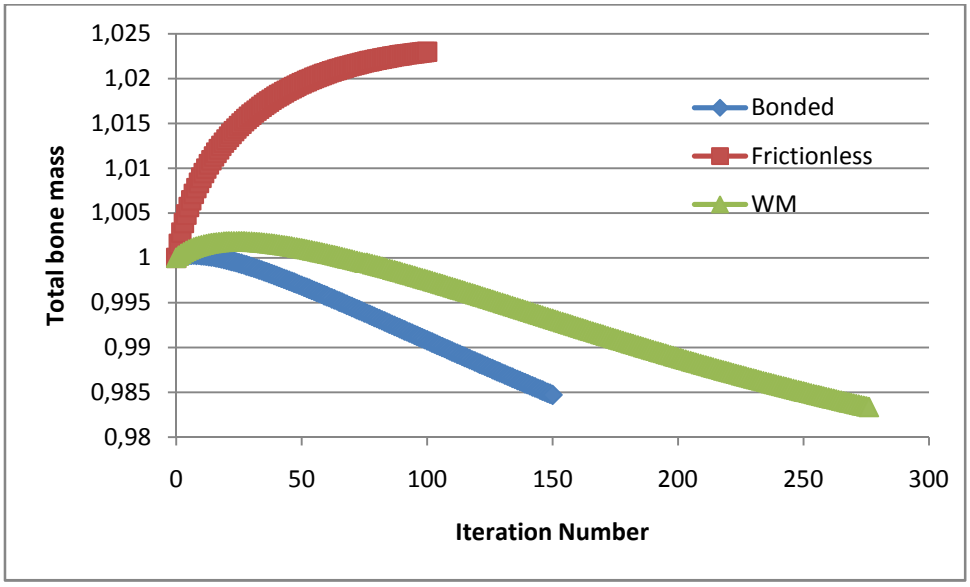

Figure 6 – Evolution of bone mass during the bone adaptation process for the press-fit models. WM corresponds to the model without muscle action.

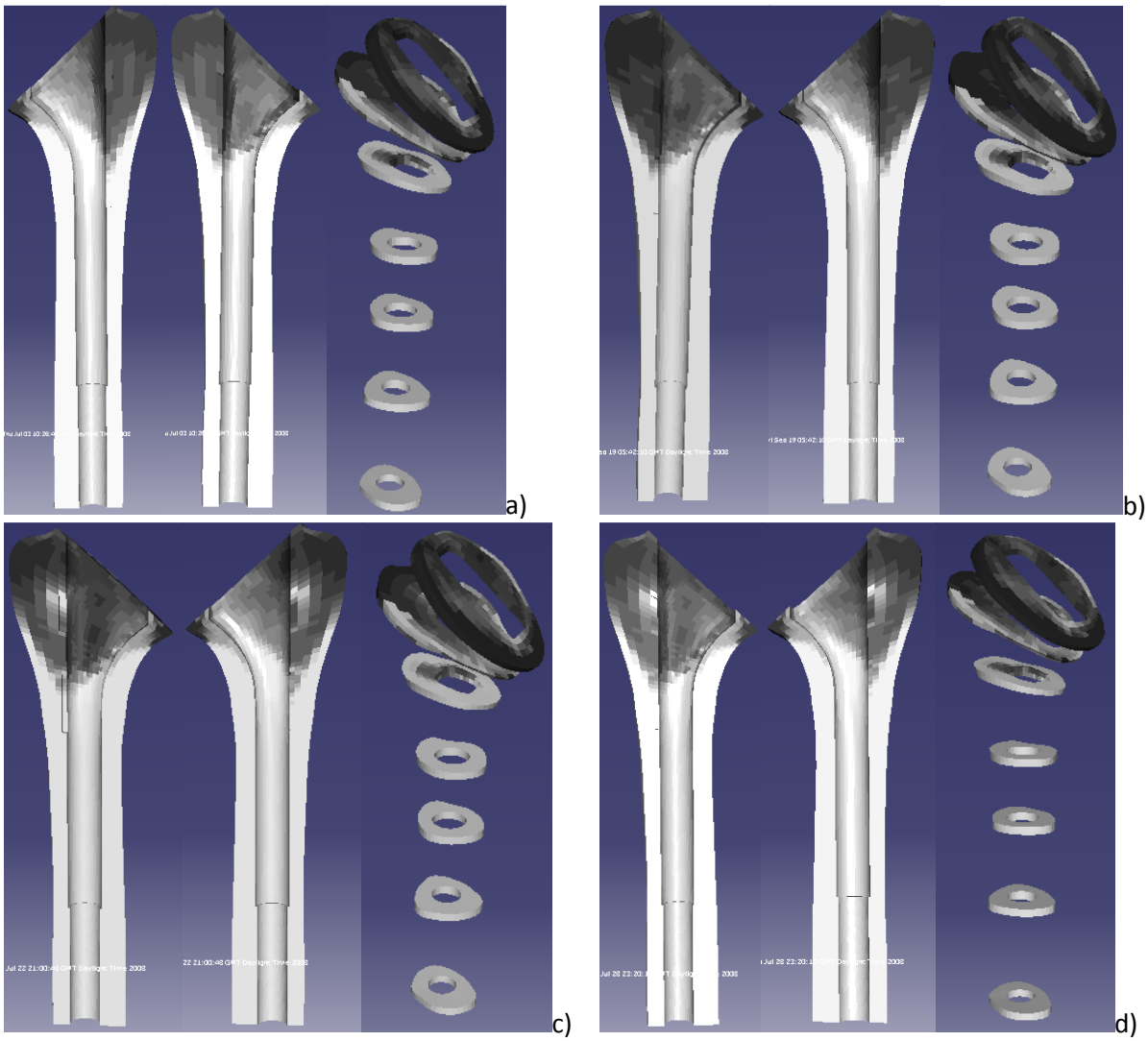

Figure 7 – Three-dimensional model of the cemented model. Densities presented in a gray scale, where gray is trabecular bone and white cortical bone. a) Initial distribution b) Bonded model final distribution c) Final distribution of the model with frictionless contact d) Final distribution of the model with friction contact

Table 1 – Relative density evolution (%) of the 8 different regions of the humerus in the three cemented models. CIE- considering interface elements. WIE – without interface elements.

	Bonded		Frictionless		Friction	
	CIE	**WIE**	**CIE**	**WIE**	**CIE**	**WIE**
Region 1	-11.609	-11.827	9.058	5.229	10.907	6.770
Region 2	-2.111	-2.167	0.396	0.004	0.820	0.278
Region 3	0.004	0.004	0.003	0.003	0.003	0.003
Region 4	0.004	0.004	0.002	0.002	0.002	0.002
Region 5	0.003	0.003	0.002	0.002	0.002	0.002
Region 6	0.051	-0.041	-0.017	-0.007	-4.838E-4	-0.002
Region 7	-2.606	-2.523	1.171	0.994	1.859	1.474
Region 8	-2.895	-2.870	1.806	1.757	2.545	2.316
Total bone mass	-1.58		1.04		1.33	

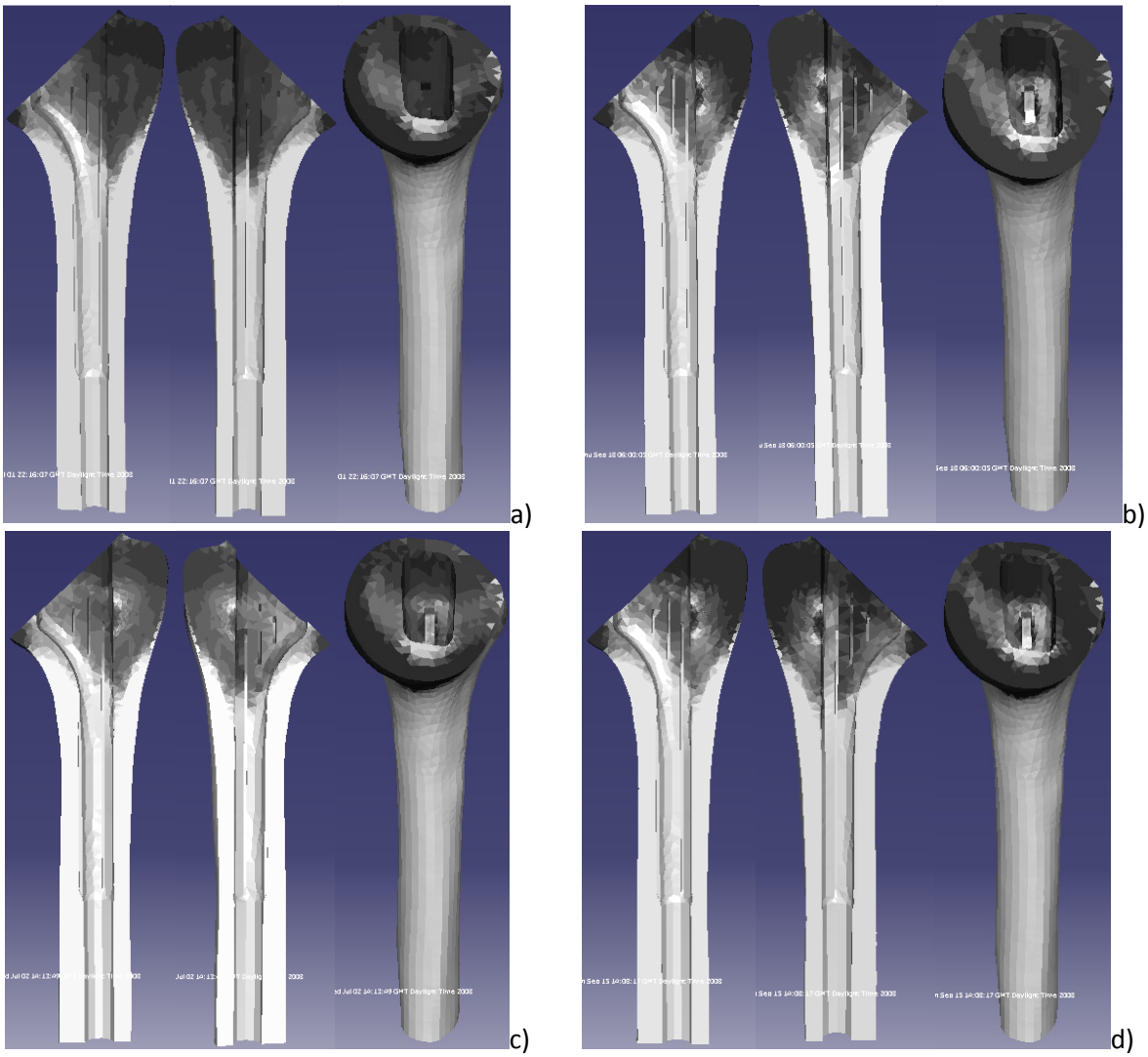

Figure 8 - Three-dimensional model of the press-fit model. Densities presented in a gray scale, where gray is trabecular bone and white cortical bone. a) Initial distribution b) Final distribution of the bonded model c) Final distribution of the model with frictionless contact d) Final distribution of the model without muscle action

Table 2 - Relative density evolution (%) of the 8 different regions of the humerus in the three press-fit models. CIE- considering interface elements. WIE – without interface elements.

	Bonded		Frictionless		Without muscle	
	CIE	**WIE**	**CIE**	**WIE**	**CIE**	**WIE**
Region 1	-8.460	-8.747	8.123	7.355	-11.074	-13.115
Region 2	-0.564	-0.515	-0.005	-0.030	2.694	2.162
Region 3	0.024	0.014	0.015	0.008	0.064	0.043
Region 4	0.009	0.007	0.006	0.004	0.019	0.017
Region 5	0.005	0.005	0.004	0.004	0.021	0.017
Region 6	0.053	0.070	0.025	0.031	0.446	0.328
Region 7	-4.595	-4.475	0.581	0.300	-7.063	-8.163
Region 8	-4.556	-4.438	0.741	0.474	-7.608	-8.699
Total bone mass	-1.53		0.98		-1.81	

4. DISCUSSION

In order to analyze bone remodelling in the humeral component after a shoulder arthroplasty, computational models were developed.

Considering the cemented stem, three models were modelled. In the bonded model, four regions presented bone loss resulting from stress shielding due to the high rigidity of the stem. In the model of frictionless contact the results are quite different, showing no bone loss (even though region 6 presents a negative evolution, its value is negligible), since the contact at the stem-cement interface does not allow for normal and shear stresses to be transmitted, causing a greater request of the bone. Indeed, it is even possible to observe an increase of bone mass in region 1. The model of friction contact, the most relevant one (Mann, et al. 1991), presents the same evolution as the model of frictionless contact.

With the press-fit stem three different models were developed. Like in the cemented models, the bonded model shows significant differences with the model of frictionless contact. The first one looses bone mass in four regions of the humerus while the last does not present any bone loss. The results from the model without muscle action present bone loss in three regions of the humerus, thus showing some stress shielding effect.

To sum up, the obtained results did not show significant bone loss which denies stress shielding and consequent bone remodelling as the main factor for the failure of shoulder prosthesis in shoulder arthroplasties.

Jochem Nagels et. al. in a study of 70 shoulder arthroplasties only reported 6 patients (9%) showing stress shielding effects though none was in risk of failure. The authors suggest the size of the stem and the quality of bone at the time of surgery also as possible reasons leading to higher stress shielding effects (Nagels, Stokdijk e Rozing 2003). In another study, about a 73 year old woman subjected to a hemiarthroplasty, some bone loss was found after 4 years however nothing is known about the previously pathology and quality of the bone (Pressel, et al. 2000).

Although stress shielding plays an important role in the hip arthroplasty, the shoulder joint presents significant anatomic and biomechanic differences which may justify the different results. The hip joint is a load bearing articulation which constantly supports half of the human body while the shoulder joint is a mobility articulation where muscles and ligaments play an important role. Therefore, despite the stem insertion in the humerus canal, the muscles which balance and stabilize the joint continue to apply load to almost all humerus, thus attenuating stress shielding effects. It should be noted that the

region 1, which presents in some models an increase in bone mass, is a muscle insertion location for the muscle of the rotator cuff, the most important in the joint stabilization. The results from the model without muscle action are also in accordance with the previous statement, showing that without muscle action bone loss occurs in three regions of the humerus, which did not happen in similar models when considering the muscle action. Note though that this example is not completely valid because without muscle action the shoulder would not present any mobility and the glenohumeral reaction forces would take different intensities.

Besides muscles and ligaments importance, the humerus geometry may also be a pertinent issue for the obtained results. The femur presents at the proximal end a high level of inclination which associated with the significant lever arm produces prosthesis bending, resulting therefore in the weakening of some regions of the bone. Although the humerus also presents some inclination at the proximal end, the lever arm is significantly lower than the lever arm of the femur and the fact that the shoulder load does not present high axial components contributes to a lower bending of the prosthesis and thus a minor role of its effects in shoulder arthroplasty.

Summarizing, by the obtained results and the pointed out reasons, bone remodelling as a stress shielding consequence does not seem to be the main reason for the failure of the humeral prosthesis.

5. CONCLUSION

In the current work computational models for bone remodelling analysis, based on the finite element method, have been presented. Two main implanted models, cemented and press-fit, have been developed using firstly Solidworks 2008 and then Abaqus for the finite element discretization.

The bone remodelling results showed no significant changes in bone mass, thus denying stress shielding and the consequent bone remodelling as the main reason for the failure of the humeral prosthesis.

Several authors suggest the reasons why arthroplasties fail are multifactorial (Boshali, Wirth e Rockwood 2006) (Franta, et al. 2007) so, in the shoulder joint, other factors may also assume particular importance, such as: mechanical failures of the implant and/or bone cement, high relative displacements at the interface, introduction of wear particles at the bone–stem interface (Joshi, et al. 2000) and other issues related with the surgical procedure (Franta, et al. 2007).

As it has been said before, there is little material in literature about stress shielding and bone remodeling in the humeral component (Pressel, et al. 2000), so the developed work can be a good complement to the existing works.

ACKNOWLEDGMENT

I gratefully acknowledge the support given by IDMEC-IST, with special thanks to Professor João Folgado, PhD and Professor Paulo Fernandes, PhD, Instituto Superior Técnico. From the medical school, Faculdade de Medicina de Lisboa, I would also like to thank Professor Jacinto Monteiro, PhD, by the support given.

REFERENCES

Andreykiv, A., P. J. Prendergast, F. van Keulen, W. Swieszkowski, e P. M. Rozing. “Bone ingrowth simulation for a concept glenoid component design.” *Journal of Biomechanics* (Elsevier Ltd.) 38 (2005).

Bigliani, Louis U., e Evan L. Flatow. *Shoulder Arthroplasty.* New York: Springer, 2005.

Boshali, Kamal I., Michael A. Wirth, e Charles A. Rockwood. “Complications of Shoulder Arthroplasty.” *Journal of Bone and Joint Surgery* 88 (2006): 2279-2292.

Favre, Philippe, Ralph Sheikh, Sandro F. Fucentese, e Hilaire A. C. Jacob. “An algorithm for estimation of shoulder muscle forces for clinical use.” *Clinical Biomechanics* 20, n.º 8 (2005): 822-833.

Fernandes, P. R., J. Folgado, C. Jacobs, e V. Pellegrini. “A contact model with ingrowth

control for bone remodelling around cementless stems." *Journal of Biomechanics* 35, n.º 2 (2002): 167.

Fernandes, P., H. Rodrigues, e C. Jacobs. "A model of bone adaptation using a global optimisation criterion based on the trajectorial theory of wolff." *Computer Methods in Biomechanics and Biomedical Engineering* 2, n.º 2 (1999): 125-138.

Folgado, João. "Modelos computacionais para análise e projecto de próteses ortopédicas." PhD Thesis, 2004.

Franta, Amy K., Tim R. Lenters, Doug Mounce, Blazej Neradilek, e Frederik A. Matsen. "The complex characteristics of 282 unsatisfactory shoulder arthroplasties." *Journal of Shoulder and Elbow Surgery* 16 (2007): 555-562.

Guedes, José Miranda, e Noboru Kikuchi. "Preprocessing and postprocessing for materials based on the homogenization method with adaptive finite element methods." (Elsevier Sequoia S. A.) 83, n.º 2 (1990): 143-198.

Hasan, Samer S., Jordan M. Leith, Barry Campbell, Ranjit Kapil, Kevin L. Smith, e Frederik A. Matsen. "Characteristics of unsatisfactory shoulder arthroplasties." *Journal of Shoulder and Elbow Surgery* 11 (2002): 431-441.

Huiskes, Rik, Harrie Weinans, e Michel Dalstra. "Adaptive Bone Remodeling and Biomechanical Design Considerations for Noncemented Total Hip Arthroplasty." *Orthopedics* 12, n.º 9 (1989): 1255-1267.

Jeffers, J., M. Browne, A. Lennon, P. Prendergast, e M. Taylor. "Cement mantle fatigue in total hip replacement: Experimental and computational testing." *Journal of Biomechanics* (Elsevier Ltd.) 40, n.º 7 (2007): 1525-1533.

Joshi, Makarand G., Suresh G. Advani, Freeman Miller, e Michael H. Santare. "Analysis of a femoral hip prosthesis designed to reduce stress shielding." *Journal of Biomechanics* 33, n.º 12 (2000): 1655-1662.

Mann, K. A., D. L. Bartel, T. M. Wright, e A. R. Ingraffea. "Mechanical Characteristics of the stem-cement interface." *Journal of Orthopaedic Research*, 1991: 798-808.

Mann, Kenneth A., David C. Ayers, e Timothy A. Damron. "Effects of Stem Length on Mechanics of the Femoral Hip Component after Cemented Revision." *Journal of Orthopaedic Research* 15 (1997): 62-68.

Nagels, Jochem, Mariëlle Stokdijk, e Piet M. Rozing. "Stress shielding and bone resorption in shoulder arthroplasty." *Journal of Shoulder and Elbow Surgery* (Elsevier Ltd.) 12, n.º 1 (2003): 35-39.

Norris, Tom R., e Joseph P. Iannotti. "Functional outcome after shoulder arthroplasty for primary osteoarthritis: A multicenter study." *Journal of Shoulder and Elbow Surgery* 11, n.º 2 (2002): 130-135.

Palastanga, Nigel, Derek Field, e Roger Soames. *Anatomia e movimento humano.* 3rd Edition. Editora Manole, Ltda, 2000.

Pressel, T., M. Lengsfeld, R. Leppek, e J. Schmitt. "Bone remodelling in humeral arthroplasty: follow-up using CT imaging and finite element modeling - an in vivo case study." *Arch Orthop Trauma Surg*, 2000: 333-335.

Sanchez-Sotelo, Joaquin, Shawn W. O'Driscoll, Michael E. Torchia, Robert H. Cofield, e Charles M. Rowland. "Radiographic assessment of cemented humeral components in shoulder arthroplasty." *Journal of Shoulder and Elbow Surgery* (Elsevier Ltd.) 10, n.º 6 (2001): 526-531.

Souza, Romeu Rodrigues. *Anatomia Humana.* 1st Edition. Editora Manole, Ltda, 2001.

Verborgt, Olivier, Rami El-Abiad, e Dominique F. Gazielly. "Long-Term results of uncemented humeral components in shoulder arthroplasty." *Journal of Shoulder and Elbow Surgery* 16, n.º 3 (2007): S13-S18.